

Epoxidized Natural Rubber/Epoxy Blends: Phase Morphology and Thermomechanical Properties

Viju Susan Mathew,¹ Soney C. George,² Jyotishkumar Parameswaranpillai,³ Sabu Thomas^{4,5,6,7}

¹Department of Chemistry, St. Thomas College, Kozhencherry, Kerala 689641, India

²Department of Basic Science, Amal Jyothi College of Engineering, Koovapally P. O., Kottayam, Kerala 686518, India

³Department of Polymer Science and Rubber Technology, Cochin University of Science and Technology, Cochin 682022, Kerala, India

⁴School of Chemical Sciences, Mahatma Gandhi University, Priyadarshini Hills, Kottayam, Kerala 686560, India

⁵Centre for Nanoscience and Nanotechnology, Mahatma Gandhi University, Priyadarshini Hills, Kottayam, Kerala 686560, India

⁶Universiti Teknologi Majlis Amanah Rakyat, Faculty of Applied Sciences, 40450, Shah Alam, Selangor, Malaysia

⁷Center of Excellence for Polymer Materials and Technologies, Tehnoloski Park 24, 1000, Ljubljana, Slovenia

Correspondence to: J. Parameswaranpillai (E-mail: jyotishkumarp@gmail.com); Sabu Thomas: (E-mail: sabupolymer@yahoo.com)

ABSTRACT: Epoxidized natural rubbers (ENRs) were prepared. ENRs with different concentrations of up to 20 wt % were used as modifiers for epoxy resin. The epoxy monomer was cured with nadic methyl anhydride as a hardener in the presence of *N,N*-dimethyl benzyl amine as an accelerator. The addition of ENR to an anhydride hardener/epoxy monomer mixture gave rise to the formation of a phase-separated structure consisting of rubber domains dispersed in the epoxy-rich phase. The particle size increased with increasing ENR content. The phase separation was investigated by scanning electron microscopy and dynamic mechanical analysis. The viscoelastic behavior of the liquid-rubber-modified epoxy resin was also evaluated with dynamic mechanical analysis. The storage moduli, loss moduli, and $\tan \delta$ values were determined for the blends of the epoxy resin with ENR. The effect of the addition of rubber on the glass-transition temperature of the epoxy matrix was followed. The thermal stability of the ENR-modified epoxy resin was studied with thermogravimetric analysis. Parameters such as the onset of degradation, maximum degradation temperature, and final degradation were not affected by the addition of ENR. The mechanical properties of the liquid-natural-rubber-modified epoxy resin were measured in terms of the fracture toughness and impact strength. The maximum impact strength and fracture toughness were observed with 10 wt % ENR modified epoxy blends. Various toughening mechanisms responsible for the enhancement in toughness of the diglycidyl ether of the bisphenol A/ENR blends were investigated. © 2013 Wiley Periodicals, Inc. *J. Appl. Polym. Sci.* 2014, 131, 39906.

KEYWORDS: morphology; phase behavior; properties and characterization; thermogravimetric analysis (TGA); thermosets

Received 30 April 2013; accepted 26 August 2013

DOI: 10.1002/app.39906

INTRODUCTION

Epoxy resins are important industrial polymers. As a result of their superior properties, for example, their ease of processing and long pot life period, epoxy resins are finding increasing use in a wide range of engineering applications, many of which involve high-value-added products.^{1,2} For many end uses, it is necessary to add other components to the resin to improve its properties. The cured epoxy products have good physical strength, dimensional stability, and excellent moisture, solvent, and chemical resistance. However, cured epoxy resins have a relatively poor toughness, which limits their applications in more

demanding areas, such as the aerospace and electronics industries. Toughening can be done with the incorporation of a small amount of elastomers as a discrete phase of microscopic particles embedded in the continuous rigid epoxy matrix.^{3,4} The pivotal work of McGarry and coworkers^{5,6} with epoxy resins modified with various functionalized butadiene-acrylonitrile rubbers yielded significant improvement in the toughness. Ramaswamy et al.⁷ studied the toughening effect of epoxidized hydroxyl-terminated polybutadiene (EHTPB) on epoxy resins cured with an amine. They obtained an enhanced lap shear strength and T-peel strength with the EHTPB content up to 10 phr, and this was attributed to the higher toughness produced

Additional Supporting Information may be found in the online version of this article.

© 2013 Wiley Periodicals, Inc.

Table I. Characteristics of ISNR-5L

Specification	ISNR-5L	Sample used
Dirt content (% maximum)	0.10	0.08
Volatile matter (%)	0.8	0.6
Ash content (%)	0.75	0.62
Wallace plasticity (minimum)	30	43
Plasticity retention index (minimum)	60	68
Mooney viscosity (ML ₁₊₄ at 120°C)	—	65–70

by the dispersed rubber particles. However, at higher EHTPB contents, the rubber phase became continuous, and a flexibilization effect dominated the toughening effect of the rubber. Studies by Kinloch and Hunston⁸ and Kishi et al.⁹ provided a detailed description of the effects of the matrix properties on fracture energy. The toughness of a rubber-modified epoxy depends on the morphology of the cured resin, and this is related to the solubility of the rubber in the uncured resin.¹⁰ Riew et al.¹¹ and Bascom et al.¹² showed that the addition of bisphenol A to a diglycidyl ether of bisphenol A (DGEBA)/carboxyl-terminated (butadiene-co-acrylonitrile) (CTBN) resin formulation increased the toughening effect of the rubber.

Recently, we¹³ used various contents of hydroxyl-terminated polybutadiene to toughen epoxy resin based on DGEBA with an anhydride hardener. The elastomeric nature of the rubber caused a reduction in the tensile strength, but the fracture toughness values increased, and we attained a maximum for 10-phr inclusion. In other studies,^{3,4} we used different concentrations of hydroxylated liquid natural rubber (NR) as a modifier for epoxy resin. Secondary phase separation was observed in the case of higher concentrations of liquid NR. Elastomer particles having a diameter of a few micrometers dispersed in the epoxy matrix were effective modifiers. We learned that hydroxyl terminated liquid natural rubber (HTLNR) droplets acted as stress concentrators; this led to the plastic deformation in the surrounding matrix and took up a significant amount of applied stress.

Dynamic mechanical analysis (DMA) measures the stiffness and damping properties of a material;¹⁴ these properties are often described as the ability to recover from deformation and the ability to lose energy as heat (damping).¹⁵ DMA is the most sensitive technique for monitoring relaxation events, such as glass transition, as the mechanical properties change dramatically when relaxation behavior is observed.¹⁶ Such studies enable the determination of the temperature dependencies of the dynamic modulus, stress relaxation, mechanical loss, and damping phenomena.¹⁷ Indeed, the influence of stoichiometry or the extent of curing on the cross-link density and glass-transition temperature (T_g) has often been studied and reported in the literature.^{18–21}

Epoxidized natural rubbers (ENRs) with different concentrations are used as modifiers for epoxy resin. The purpose of this study was to develop a high-performance material with epoxy resin and liquid NRs. The variations in the dynamic mechanical properties of the blends were correlated with the morphological aspects. The thermal and mechanical behaviors of the liquid-NR-modified epoxy resin were explored. We observed that the degradation pattern remained the same for both the neat epoxy

and the ENR/epoxy blends. It is also important to add that although the modification of the epoxies by synthetic rubber has been extensively reported, so far no serious attempts have been made with liquid NR. The easy availability of this NR and its comparatively low cost favor the preparation of epoxy/NR blends. In view of this, a detailed investigation was carried out to examine the morphology and thermal and mechanical properties of epoxy/liquid NR blends.

EXPERIMENTAL

NR

Natural crumb rubber (Indian Standard Natural Rubber ISNR-5L), having a number-average molecular weight (M_n) of 820,000 g/mol and an intrinsic viscosity in benzene at 30°C of 445 dL/g, was supplied by the Rubber Research Institute of India (Kottayam). The characteristics of ISNR-5L are given in Table I. It was used to synthesize the ENRs.

Epoxy Resin

An unmodified bisphenol A based epoxy resin (LAPOX B-11), supplied by Atul Polymers India, Ltd. (Gujarat), was used. It was a medium-viscosity resin used mainly for solvent-free coatings and building applications. LAPOX B-11 had an epoxide index of 5.2–5.5 equiv/kg, an epoxide equivalent of 182–192 g/equiv, and a viscosity of 9000–12,000 mPa s at 25°C. The characteristics of the epoxy resin are depicted in Table II.

Other Additives

Nadic methyl anhydride (K 68) supplied by Atul was used as the curing agent. *N,N*-Dimethyl benzyl amine, also supplied by Atul, was used as the accelerator. The resin, the hardener, and the accelerators were mixed in a ratio of 100:80:1 w/w. H₂O₂ (30 wt %) and toluene were supplied by E. Merck (India).

EXPERIMENTAL

Preparation of the ENRs

NR can be epoxidized in solution or in the latex stage by peracids.^{22–26} An amount of 100 g of rubber was made into a solution in toluene in a three-necked, round-bottomed flask equipped with a thermometer, mechanical stirrer, and condenser. A volume of 40 mL of acetic acid was added; this was followed by 10.6 g of sodium acetate to maintain the pH at 5. Then, 75 mL of H₂O₂ (30% w/v) was added dropwise to the solution over a period of 1 h. The contents were stirred continuously for another 4 h at room temperature. The products were washed repeatedly with distilled water in a separating funnel to

Table II. Characteristics of the Epoxy Resin

Property	Epoxy resin
M_n	374 g/mol
Degree of polymerization	0.12
Epoxy value	5.3 equiv/kg
Viscosity at 25°C	9000–12,000 mPa s
Density at 25°C	1.18 g/cm ³
Solubility parameter	20.9 MPa ^{1/2}
T_g	–17°C

Table III. Characteristics of the ENR

Characteristic	ENR
Hydroxyl value (mg of KOH/g of rubber)	13.01 mg/g
Epoxy value (mg of KOH/g of rubber)	16.23 mg/g
Acid number (mg of KOH/g of rubber)	2.21 mg/g
Iodine value (mg of Na ₂ S ₂ O ₃ /g of rubber)	168 mg/g
Functionality	1.84
Viscosity-average molecular weight	14,679 g/mol
T_g	-33°C
M_n	8065 g/mol
Weight-average molecular weight	47,350 g/mol
Polydispersity index	5.8

remove the acid. They were dried in a vacuum oven at 40°C. The samples were analyzed with various experimental methods. The results are given in Table III.

Characterization of the ENRs

Gel Permeation Chromatography (GPC) Analysis. GPC provides a quick and efficient method for polymer fractionation and the computation of the molecular weight distribution curve. A Waters 410 differential refractometer in association with a Waters 510 pump was used to determine the molecular weight. Ultra Styragel columns having pore sizes of 50, 100, and 1000 nm and operated with tetrahydrofuran at 1 mL/min were used. The data acquisition was done by a UV absorbance detector set at 254 nm and a differential refractive-index detector. The typical sample concentration was 0.2 wt %, and the instrument was calibrated with polystyrene standards with a peak molecular weight of about 32,500.

IR Analysis. The IR spectrum of ENR was taken in a Nicolet Magna-560 FTIR spectrometer with chloroform as the solvent. A calibration curve was prepared with 1,4-butanediol at different concentrations.

¹H-NMR Analysis. The ¹H-NMR spectrum of the ENR sample was recorded in CDCl₃ with a Bruker DPX 300 Fourier transform NMR spectrometer operating at 300 MHz.

Preparation of the Blends. Blends with 5, 10, 15, and 20 wt % rubber were prepared. Epoxy resin/liquid rubber blends were prepared in the following manner. Epoxy resin and rubber were degassed separately in a vacuum oven for 30 min. The epoxy resin and the required amounts of rubber were thoroughly stirred in a silicon oil bath at 100°C for 20 min to get a homogeneous system. Nadic methyl anhydride was added in stoichiometric amounts with stirring, and this was followed by the addition of the catalyst, a tertiary amine.

We performed the curing by pouring the mixture into a greased Teflon mold. It was then precured for 30 min at 120°C, and this was followed by 6 h of curing at 180°C and 2 h of postcuring at 200°C.

Characterization of the ENR/Epoxy Blends

DMA. Dynamic mechanical measurements were performed from -100 to 200°C at a frequency of 10 Hz and a heating rate

of 3°C/min with a DMA Q 800 equipped with a three-point bending device with a 44-mm span. The specimens used for dynamic mechanical tests were machined to 60 × 12 × 10 mm³ from the previous plates.

Thermogravimetric Analysis (TGA). The thermal stability of the blends was determined with TGA. A thermal analyzer (Netzsch TG 209 with an Al₂O₃ crucible) was used to heat the samples in an N₂ atmosphere to 700°C at a heating rate of 20°C/min.

Fracture Toughness and Fracture Energy. The fracture toughness of the specimens was determined according to ASTM STP410. Rectangular specimens 110 mm in length, 35 mm in width, and 3 mm in thickness were used for fracture toughness measurements. Fracture toughness or critical stress intensity factor (K_{IC}) values were determined with precracked, single-edge-notched specimens in tension mode with a span of 50 mm. A notch of 5 mm was made at one edge of the specimen. We made a natural crack by pressing a fresh razor blade into the notch. Fracture toughness was determined from the load–displacement curve when the loading was increased monotonously with a tensile tester from the load–elongation ($F-\Delta l$) response of the single edge notched tension (SEN-T) specimens with eq. (1):

$$K_{IC} = (F_{max}/BW^{1/2}) f(a/W) \quad (1)$$

where B is the thickness of the specimens, W is the width of the specimens, a is the crack length, F_{max} is the maximum force in the $F-\Delta l$ trace and $f(a/W)$ is the geometry correction factor and is represented as follows:

$$f(a/W) = 1.99 - 0.41(a/W) + 18.7(a/W)^2 - 38.48(a/W)^3 + 53.85(a/W)^4 \quad (2)$$

The fracture energy or critical strain energy release rate (G_{IC}) was estimated from K_{IC} with eq. (2):

$$G_{IC} = \frac{(1-\nu)^2 K_{IC}^2}{E} \quad (3)$$

where ν is Poisson's ratio and E is the elastic modulus.

Impact Strength. The Izod impact test was performed according to ASTM D-256 with a hammer length of 0.33 m at room temperature. Rectangular specimens with dimensions of 60 × 12 × 2 mm³ were used. The values were taken from an average of six specimens.

Fracture Surface Analysis. The morphology of the fractured surface of the crosslinked epoxy and epoxy blends were examined with an ULTRA field emission scanning electron microscope (Ultra Plus model, Nano Technology Systems Division Carl Zeiss SMT AG, Germany). The fractured samples were coated with platinum by vapor deposition with a vacuum sputter.

RESULTS AND DISCUSSION

Characterization of ENR

IR Analysis. The IR spectrum of ENR is depicted in Figure 1. It was well documented in the literature that ring opening occurred during the epoxidation of NR.^{27,28} The presence of the hydroxyl group was indicated by the broad peak in the region

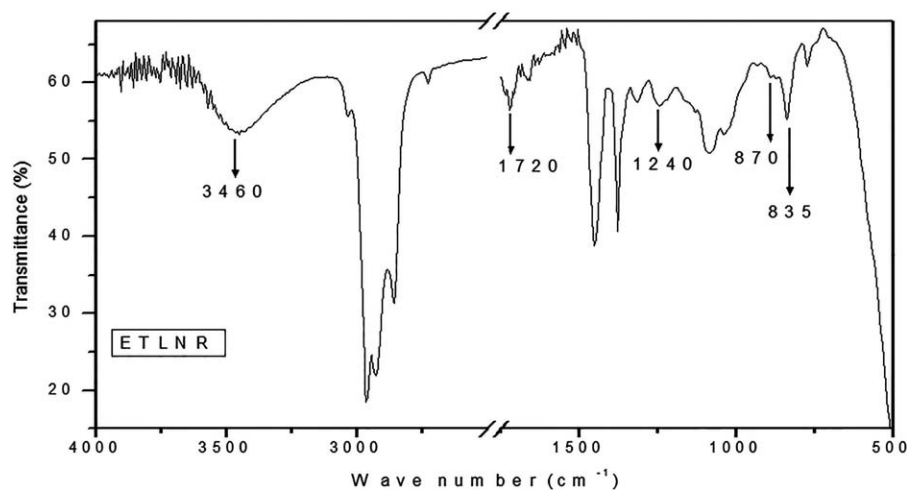


Figure 1. IR spectrum of epoxidized natural rubber (ENR).

of 3460 cm^{-1} , and the absorption peak of the epoxide ring occurred at 1240 and 870 cm^{-1} . Similar observations were reported for ENR.²⁹ This showed that the product had both epoxy and hydroxyl groups and indicated that the C=C bonds underwent epoxidation and hydroxylation.^{30,31} The prominent IR frequencies of the ENRs are represented in Table IV.

NMR Analysis. The peak positions obtained from the $^1\text{H-NMR}$ spectrum of ENR are represented in Table V. The resonances at 1.68, 2.03, and 5.11 ppm were characteristic of isoprene units. The signal at 1.3 ppm was mainly due to the secondary hydroxyl group. The peak at 2.71 ppm was attributed to the appearance of the methine resonance due to the proton attached to the oxirane ring ($-\text{CH}-^5$). These results were in agreement with those of recent work by Yokshan³⁰ and Hamzah et al.³² The similarity of these spectra with those of NR confirmed that the *cis*-1,4-polyisoprene structure was retained in the liquid NR.³³

GPC Analysis. GPC analysis gave M_n . The chromatogram obtained from the Waters 410 differential refractometer is given in Figure 2. The peak corresponded to an M_n of 8065.

Table IV. Prominent IR Frequencies of the ENR

Peak position (cm^{-1})	Characteristic groups
3460	Broad $-\text{OH}$ stretching
3040	m, C-H stretching
2961	s, C-H asymmetric stretching, $-\text{CH}_2$
2850	s, C-H symmetric stretching, $-\text{CH}_3$
1707	m, $\text{C}=\text{C}$ and <i>cis</i> -vinylene
1447	s, C-H asymmetric def $-\text{CH}_3$
1375	s, C-H symmetric def $-\text{CH}_3$
1240	Characteristic band of the epoxy group
1060	m, C-O str aliphatic primary alcohol
870	Characteristic band of the epoxy group
835	s, C-H out-of-plane def in $\text{CHR}=\text{CCR}'$

Def, deformation; Str, stretching.

Characterization of the ENR/Epoxy Blends

DMA of the ENR/Epoxy Blends. The viscoelastic properties of the ENR/epoxy blends were studied with DMA. The variation of the storage modulus (E') with respect to the temperature is recorded in Figure 3. The unmodified crosslinked epoxy resin and the crosslinked epoxy blends showed only one inflection point, which was at the T_g of the crosslinked epoxy. A sharp decrease in E' was observed for all of the blends near the glass transition of the epoxy network. E' decreased with increasing temperature. In general, the E' values for the blends were lower than that of the neat epoxy system. This was due to the presence of less stiff ENR.³⁴ It was interesting to note that the T_g of the epoxy phase shifted slightly toward the low-temperature side with the addition ENR. The decrease in T_g was an indication of a corresponding decrease in the crosslinking density and was due to the dilution effect by the addition of ENR or to the presence of miscible ENR in the epoxy phase.³⁵

The plot of $\tan \delta$ versus the temperature of the ENR-modified epoxy is given in Figure 4. The T_g values of the fully cured epoxies were taken to be the temperatures at the maximum of the $\tan \delta$ peaks. The T_g values of the blends are given in Table VI. We found that the T_g of the epoxy resin decreased when it was blended with ENR and was more significant for higher weight percentages of ENR. The different peak heights indicated that the damping properties of the toughened blends were different. The magnitude of $\tan \delta_{\text{max}}$ was at a minimum for the blends because of an epoxy phase decrease in size with the

Table V. Peak Assignments in the $^1\text{H-NMR}$ Spectrum of ENR

Peak position (ppm)	Characteristic group
1.3	$\text{CH}-\text{CO}$
1.7	s, $\text{CH}-\text{C}=\text{C}$
2.0	s, $\text{H}_2\text{C}-\text{C}=\text{C}$
2.7	
5.1	m, $-\text{C}=\text{C}-\text{H}$

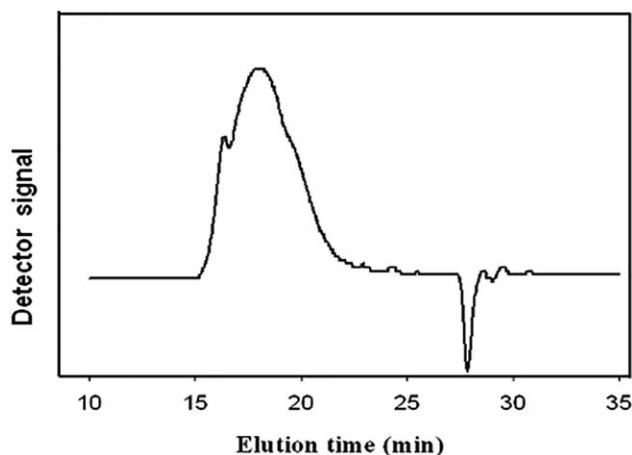


Figure 2. GPC spectrum of ENR.

addition of ENR because the dimensions of the rubber-rich phase were larger at higher ENR concentrations.³⁶

The loss modulus is a measure of the viscous response of a material. Two relaxation peaks were observed in the loss modulus curves (Figure 5). The peak around 120°C was due to the epoxy-rich phase. The relaxation peak maximum was taken as T_g ; the T_g of the epoxy phase decreased slightly with the incorporation of the rubber phase; again, the loss modulus peak height was decreased by the addition of rubber. As mentioned earlier, this was due to the epoxy phase decrease in size with the addition of ENR. A second relaxation peak at -70°C was observed, called β relaxation; this relaxation was attributed to the motions of glycidyl units in the epoxy network.

TGA. The TGA curve of ENR is shown in Figure 6(a). There were two stages of degradation: the first stage was between 220 and 350°C, and the second stage was between 500 and 630°C. The weight loss at the end of the first stage was 70%, and that at the end of the second step was over 99%. The temperature of maximum degradation (T_{max}) of the first stage occurred at

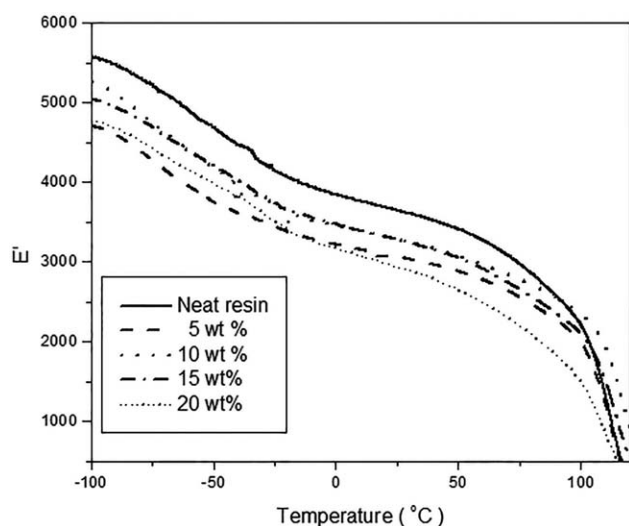


Figure 3. Variation of E' of the DGEBA/ENR blends.

Table VI. T_g Values of the Epoxy Phase from the Loss Modulus Data

Sample code	T_g from the loss modulus (°C)
Neat	118
5 wt % ENR	112
10 wt % ENR	112
15 wt % ENR	114
20 wt % ENR	109

420°C, and that of the second stage was 578°C. This initial weight loss up to 220°C was possibly due to the volatilization of impurity traces and moisture, which continued for some period at a very slow rate. As the actual decomposition began at elevated temperatures, the weight loss occurred at a faster rate. The main degradation step corresponded to the breaking down of the polymer chains into volatile fragments.

The thermal stability of the neat epoxy and ENR/epoxy blends was analyzed with TGA in an N_2 atmosphere. TGA and derivative thermogravimetry (DTG) curves for all of the crosslinked blends are given in Figure 6(b,c), respectively. We observed that a single-stage thermal decomposition was evident in the TGA. The average weight loss of around 1–2% up to 250°C was due to the release of moisture. On the other hand, the weight loss before 300°C was related to the decomposition of the polymer. The initial decomposition temperature (IDT), final decomposition temperature (FDT), and T_{max} values for the neat epoxy and ENR blends are tabulated in Table VII. The anhydride-cured epoxy exhibited a T_{max} around 419°C and varied in the range 416–419°C in the case of the DGEBA/ENR blends with around a 50% mass loss. T_{max} was taken as the maximum in the DTG curve. Beyond the main degradation stage, all of the volatile materials were driven off from the sample, and this resulted in the residual char. The residual percentage of the blends was not as good as that of the neat epoxy because of the

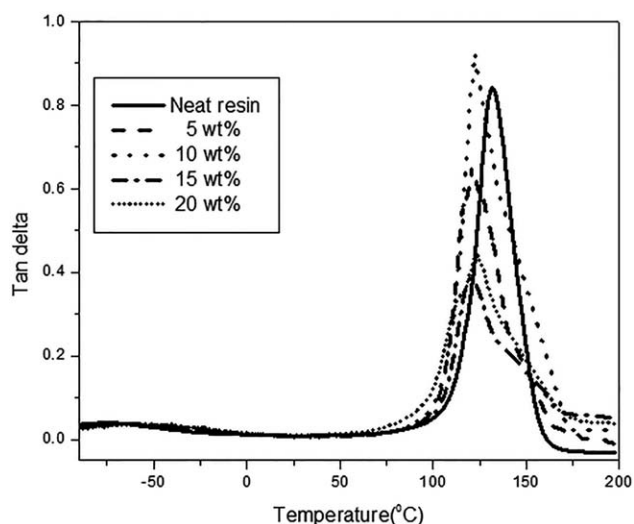


Figure 4. Variation of $\tan \delta$ with the temperature of the DGEBA/ENR blends.

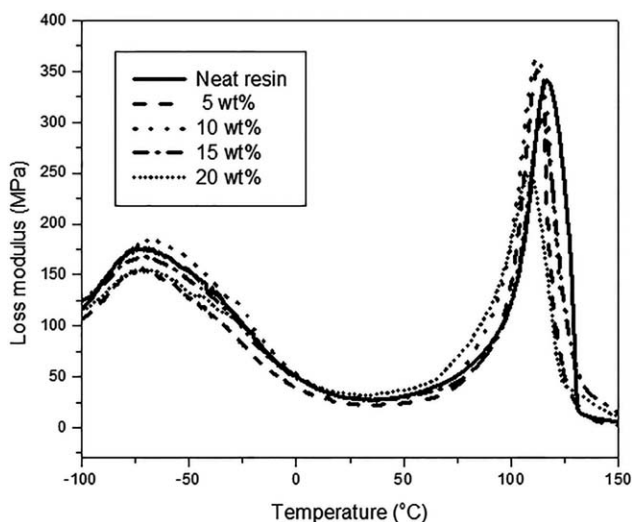


Figure 5. Variation of the loss modulus with the temperature of the DGEBA/ENR blends.

presence of the less thermally stable rubber phase. On the other hand, the IDT, FDT, and T_{max} values were not affected by the blending of the epoxy with ENR.

Table VII. Thermal Properties of the Neat and ENR-Modified Epoxies

ENR content (wt %)	IDT (°C)	FDT (°C)	T_{max} (°C)
0	369	459	419
5	370	458	419
10	355	463	419
15	373	459	419
20	358	463	416

Mechanical Properties. The variation of the unnotched and notched impact strengths of the epoxy resin containing different amounts of ENR is given in Table VIII. All of the modified networks showed a higher impact resistance than the neat epoxy in both the notched and unnotched specimens. However, the property attained a maximum with a 10 wt % ENR content and decreased with increasing rubber content. The impact strength increased up to a 10 wt % rubber concentration because of the effective stress concentration and stress-transfer behavior of the phase-separated, rubber-rich particles, which amplified the plastic deformation of the highly brittle matrix to a certain extent. The impact strength was enhanced by 305% in the case of the 10 wt % ENR modified blends. The decreasing

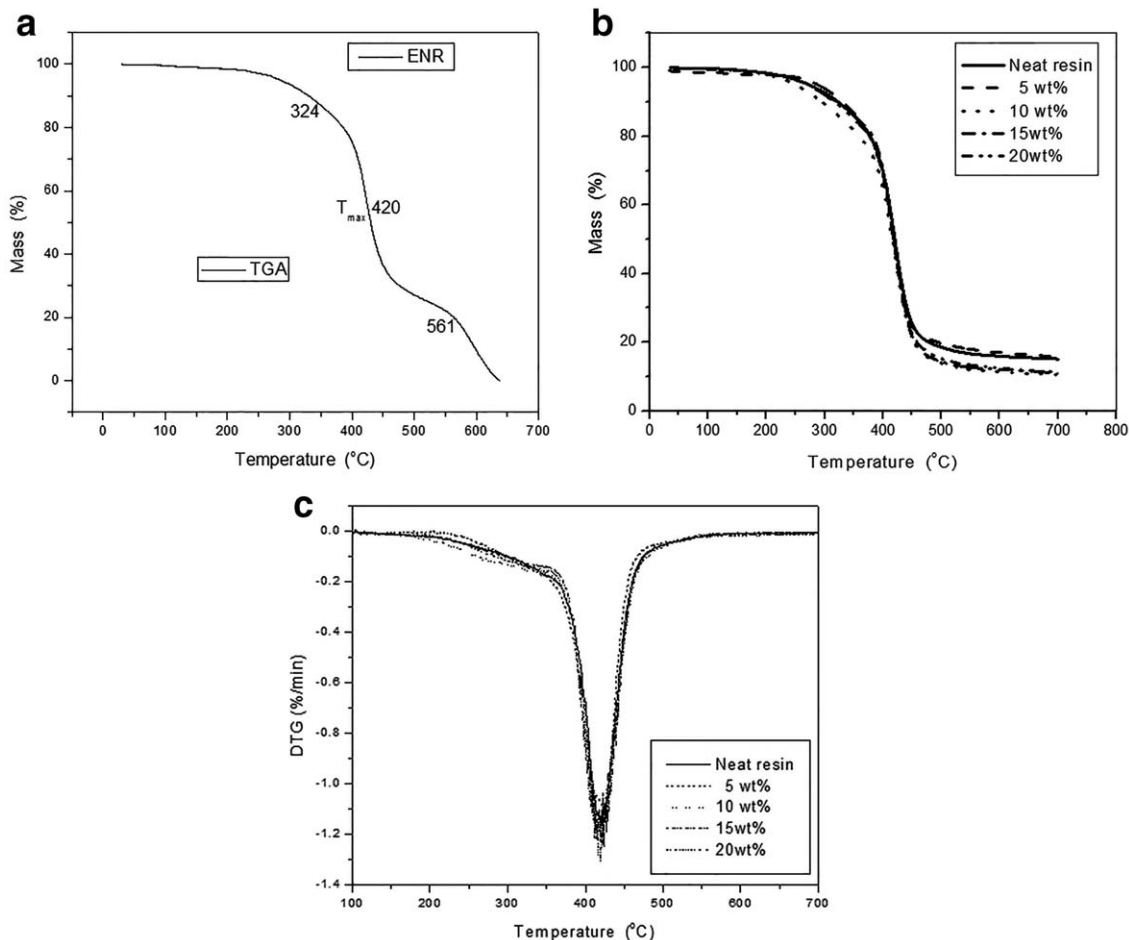
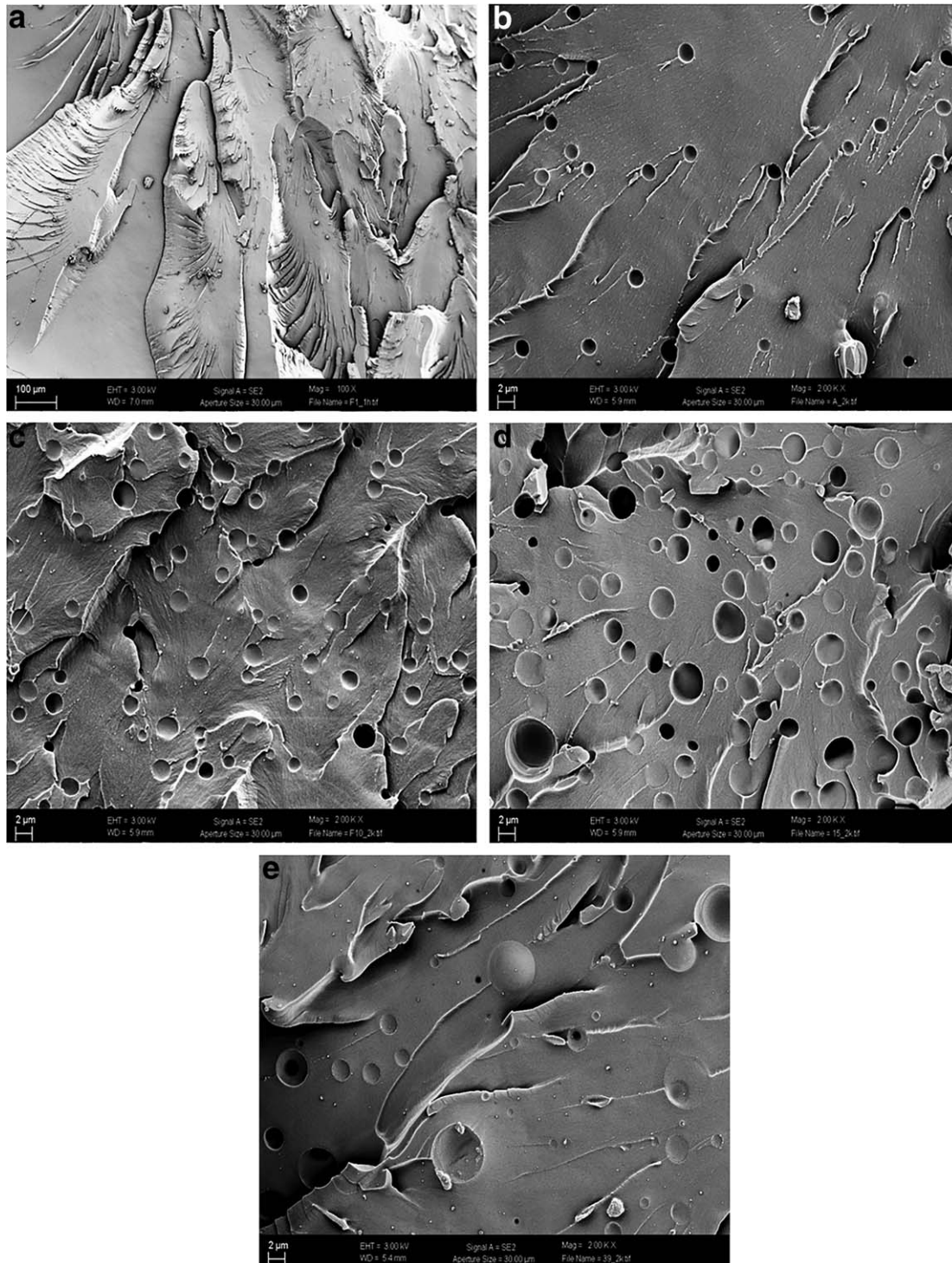


Figure 6. (a) TGA curve of ENR, (b) TGA curves of the neat epoxy and epoxy/ENR blends, and (c) DTG curves of the neat epoxy and the epoxy/ENR blends.

Table VIII. Mechanical Properties of the DGEBA/ENR Blends

Sample	G_{IC} (kJ/m ²)	K_{IC} (M/Nm ^{1/2})	Unnotched impact strength (J/m)	Notched impact strength (J/m)
Neat resin	0.5 ± 0.01	0.84 ± 0.01	6.87 ± 0.8	1.85 ± 0.1
5 wt % ENR	1.39 ± 0.02	1.84 ± 0.02	12.74 ± 0.7	2.45 ± 0.05
10 wt % ENR	2.53 ± 0.01	2.51 ± 0.03	20.98 ± 0.9	2.93 ± 0.07
15 wt % ENR	2.20 ± 0.01	2.36 ± 0.02	18.22 ± 0.7	2.78 ± 0.05
20 wt % ENR	2.11 ± 0.03	1.79 ± 0.03	16.59 ± 0.6	2.55 ± 0.06

**Figure 7.** Scanning electron micrographs of the (a) neat epoxy and (b) 5, (c) 10, (d) 15, and (e) 20 wt % ENR/epoxy blend surfaces after fracture measurements.

tendency of the impact strength after a maximum value at 10 wt % ENR inclusion was attributed to the aggregated size of rubber particles as the concentration of rubber increased. This behavior was also observed in other rubber-modified epoxy systems.^{37,38} The large elastomeric domains acted as deflection sites and led to the catastrophic failure of the matrix. The impact strength of the 20 wt % ENR blend was higher than that of neat epoxy; this could have been due to matrix ductility and the reduction in crosslinking density attained by the incorporation of rubber. The impact strength depended on the matrix ductility as explained in certain rubber-modified epoxy works.^{39,40} The unnotched samples were found to have a higher impact strength than the notched ones because more energy was required to initiate crack and crack propagation.

The effects of the rubber concentration on the fracture toughness and fracture energy are given in Table 8. Both the K_{IC} and G_{IC} values reached a maximum value in the 10 wt % ENR modified blends. This was attributed to the smaller rubber domains uniformly distributed in the epoxy matrix and was evident from the scanning electron micrographs shown in Figure 7. About a 300% enhancement in the fracture toughness was achieved by the addition of 10 wt % ENR to the epoxy matrix. The improvement in the toughness of the ENR systems was due to the reduction in the crosslinking density and, to a lesser extent, to flexibilization. The increase in the fracture toughness behavior of the ENR/epoxy samples showed a better energy-transfer mechanism operating in the ENR-modified epoxy because of the excellent interfacial adhesion and bonding with the matrix.

The fracture surface of the ENR/epoxy blends is shown in Figure 7(a–e). For the neat epoxy system, the cracks spread freely and regularly and oriented in the direction of loading; this suggested typical characteristics of brittle fracture, as revealed by Figure 7(a).⁴¹ The scanning electron micrographs of the fracture surfaces of the cured blends containing 5–20 wt % ENR are shown in Figure 7(b–e). Matrix droplet morphology was observed (the rubber particles were dispersed in the epoxy matrix) for all of the blends studied. However, the domain size increased with increasing ENR content. It is important to mention that the rubber phase in the epoxy matrix had to be hardened during curing. The fracture toughness first increased and then decreased for the cured blends; a maximum fracture toughness of 2.51 M/Nm^{1/2} was obtained with the 10 wt % ENR modified blends. The smaller rubber particles were difficult to cavitate or debonded from the epoxy matrix and hence better toughness for 10 wt % ENR modified blends.⁴² The interface between the epoxy phase and the rubber phase remained intact. This was evidence for good adhesion between the matrix and the dispersed domains. Hence, the stress was transferred more effectively to the rubber domains from the crosslinked epoxy phase. In addition, the rubber particle was considered to bridge or pin the crack as it propagated through the material.⁴³ Thus, the rubber particles were able to prevent the crack from growing to a catastrophic size. Thus, the increase in toughness was due to the amount of elastic energy stored in the rubber particles during applied loading; the deformation of the rubber particles in the matrix could have been responsible for the enhanced stress transfer and, hence, the toughness.

CONCLUSIONS

Toughening epoxy resins with functionalized reactive liquid rubbers has been a subject of interest for many investigators. The morphology and mechanical and dynamic mechanical properties of ENR/epoxy blends was analyzed. E' and the glass transition were decreased slightly with the addition of rubber. The thermal stability of the epoxy matrix was retained by the addition of the rubber. The domain size increased with ENR content in the blends because of coalescence. For the modified specimens, the impact strength (both notched and unnotched) and fracture toughness were found to be greater than those of the unmodified epoxy. The ENR droplets acted as stress concentrators; as a result, the plastic deformation in the surrounding matrix could take up a significant amount of applied stress. The cured epoxy resin containing ENR concentrations around 10 wt % showed the best balance of properties.

ACKNOWLEDGMENTS

The authors acknowledge financial support from the Ministry of Higher Education, Science and Technology of the Republic of Slovenia (contract grant number 3211-10-000057, Center of Excellence Polymer Materials and Technologies). One of the authors (J.P.) acknowledges the Department of Science and Technology, Government of India, for financial support under an Innovation in Science Pursuit for Inspired Research (INSPIRE) Faculty Fellowship (contract grant number IFA-CH-16).

REFERENCES

1. Varma, K.; Gupta, V. B. In *Comprehensive Composite Materials*; Elsevier Science: Amsterdam, The Netherlands, **2003**; p 1.
2. Fink, J. K. In *Reactive Polymers Fundamentals and Applications*; William Andrew: Norwich, NY, **2005**; Chapter 3, p 139.
3. Mathew, V. S.; Sinturel, C.; George, S. C.; Thomas, S. *J. Mater. Sci.* **2010**, *45*, 1769.
4. Mathew, V. S.; Jyotishkumar, P.; George, S. C.; Gopalakrishnan, P.; Delbreilh, L.; Saiter, J. M.; Saikia, P. J.; Thomas, S. *J. Appl. Polym. Sci.* **2012**, *125*, 804.
5. McGarry, F. J.; Willner, A. M. Research Report R 68-6; School of Engineering, Massachusetts Institute of Technology: Cambridge, MA, **1968**.
6. Sultan, J. N.; McGarry, F. J. *Polym. Eng. Sci.* **1973**, *13*, 29.
7. Latha, P. B.; Adhinarayanan, K.; Ramaswamy, R. *Int. J. Adhes. Adhes.* **1994**, *14*, 57.
8. Kinloch, A. J.; Hunston, D. L. *J. Mater. Sci. Lett.* **1986**, *5*, 909.
9. Kishi, H.; Shi, B. Y.; Huang, J.; Yee, A. F. *J. Mater. Sci.* **1998**, *33*, 3479.
10. Jackson, M. B.; Edmond, L. N.; Varley, R. J.; Warden, P. G. *J. Appl. Polym. Sci.* **1993**, *48*, 1259.
11. Riew, C. K.; Rowe, E. H.; Siebert, A. R. *Am. Chem. Soc. Div. Org. Coat. Plast. Prepr.* **1974**, *34*, 352.

12. Bascom, W. D.; Ting, R. Y.; Moulton, R. J.; Riew, C. K.; Siebert, A. R. *J. Mater. Sci.* **1981**, *16*, 2657.
13. Thomas, R.; Yumei, D.; Yuelong, H.; Le, Y.; Moldenaers, P.; Weimin, Y.; Czigany, T.; Thomas, S. *Polymer* **2008**, *49*, 278.
14. Murayama, T.; Bell, J. P. *J. Polym. Sci.* **1970**, *8*, 437.
15. Menard, K. P.; *Dynamic Mechanical Analysis—A Practical Introduction*; CRC: Boca Raton, FL, **1999**.
16. Senich, G.; MacKnight, W. J.; Schneider, N. S. *Polym. Eng. Sci.* **1979**, *19*, 313.
17. Bana, R.; Banthia, A. K. *J. Wood Chem. Technol.* **2011**, *31*, 218.
18. Charlesworth, J. M. *Polym. Eng. Sci.* **1988**, *28*, 221.
19. Charlesworth, J. M. *Polym. Eng. Sci.* **1988**, *28*, 230.
20. Wingard, C. D.; Beatty, C. L. *J. Appl. Polym. Sci.* **1990**, *41*, 2539.
21. Won, Y.; Galy, J.; Gerard, J. F.; Pascault, J. P.; Bellenger, V.; Verdu, J. *Polymer* **1990**, *31*, 1787.
22. Greenspan, F. P. *Chemical Reactions of Polymers*; Wiley-Interscience: New York, **1964**; Chapter 2; p 154.
23. Pummerer, R.; Burkard, P. A. *Chem. Abstr.* **1923**, *17*, 898.
24. Stille, J. K. *Chem. Rev.* **1958**, *58*, 580.
25. Halasa, A. F.; Massie, J. M.; Ceresa, R. J. In *Science and Technology of Rubber*; Mark, J. E., Erman, B., Eds.; Academic, **2011**; Chapter 11; p 512.
26. Zhang, J.; Zhou, Q.; Jiang, X. H.; Du, A. K.; Zhao, T.; Kasteren, J.; Wang, Y. Z. *Polym. Degrad. Stab.* **2010**, *6*, 1077.
27. Roy, S.; Namboodri, C. S. S.; Maiti, B. R.; Gupta, B. R. *Polym. Eng. Sci.* **1993**, *33*, 92.
28. Gelling, I. R. *Rubber Chem. Technol. J.* **1985**, *58*, 86.
29. Gan, S. N.; Hamid, Z. A. *Polymer* **1997**, *38*, 1953.
30. Yoksan, R.; Kasetsart, J. (Nat. Sci.) **2008**, *42*, 325.
31. Rajaseka, R.; Pal, K.; Heinrich, G.; Das, A.; Das, C. K. *Mater. Des.* **2009**, *30*, 3839.
32. Hamzah, R.; Bakar, M. A.; Khairuddean, M.; Mohammed, I. A.; Adnan, R. *Molecules* **2012**, *17*, 10974.
33. Nirmal, S. N.; Maithi, C.; Padmavathi, T.; Vanaja, A.; Rao, R. M. V. G. K. *High Perform. Polym.* **2006**, *18*, 57.
34. George, S. M.; Puglia, D.; Kenny, J. M.; Jyotishkumar, P.; Thomas, S., submitted.
35. Jyotishkumar, P.; Pionteck, J.; Moldenaers, P.; Thomas, S. *J. Appl. Polym. Sci.* **2013**, *127*, 3159.
36. Jyotishkumar, P.; Pionteck, J.; Häßler, R.; Sinturel, C.; Mathew, V. S.; Thomas, S. *Ind. Eng. Chem. Res.* **2012**, *51*, 2586.
37. Ratna, D.; Banthia, A. K.; Deb, P. C. *J. Appl. Polym. Sci.* **2000**, *78*, 717.
38. Ratna, D. *Polymer* **2001**, *42*, 4209.
39. Ratna, D.; Banthia, A. K.; Deb, P. C. *J. Appl. Polym. Sci.* **2001**, *80*, 1792.
40. Lanzetta, N.; Laurienzo, P.; Malinconico, M.; Martuscelli, E.; Ragosta, G.; Volpe, M. G. *J. Mater. Sci.* **1992**, *27*, 786.
41. Mondragon, I.; Solar, L.; Nohales, A.; Vallo, C. I.; Gomez, C. M. *Polymer* **2006**, *47*, 3401.
42. Tian, X.; Geng, Y.; Yin, D.; Zhang, B.; Zhang, Y. *Polym. Test.* **2011**, *30*, 16.
43. Ahmad, I.; Hassan, F. M. *J. Reinf. Plast. Compos.* **2010**, *29*, 2834.